Functional characterization of the thylakoid Ndh complex phosphorylation by site-directed mutations in the *ndhF* gene

Mercedes Martín [a], Helena T. Funk [b], Patricia H. Serrot [a], Peter Poltnigg [b], Bartolomé Sabater [a],*

[a] Departmento de Biología Vegetal. Universidad de Alcalá. Alcalá de Henares, 28871-Madrid, Spain
[b] Zellbiologie, Philipps-Universität Marburg, Karl-von-Frisch-Str., 35032 Marburg, Germany

ARTICLE INFO

ABSTRACT

To investigate the phosphorylation of the NDH-F subunit of the thylakoid Ndh complex, we constructed three site-directed mutant transgenic tobaccos (*Nicotiana tabacum*) (T181A, T181S and T181D) in which the $_{541}ACT_{543}$ triplet encoding the Thr-181 has been substituted by GCT, TCT or GAT encoding alanine, serine and aspartic acid, respectively. Western blots with phospho-threonine antibody detected the 73 kD NDH-F phosphorylated polypeptide in control but not in mutant tobaccos. Differences in Ndh activity, chlorophyll fluorescence and photosynthesis among mutants and control plant demonstrate the key role of the phosphorylation of conserved Thr-181 in the activity and function of the Ndh complex. The substitution of aspartic acid for threonine in T181D mimics the presumable activation effects of the threonine phosphorylation in Ndh activity, post-illumination increase of chlorophyll fluorescence and photosynthesis rapid responses to changing light intensities. A tentative role of the phosphorylation-activated Ndh complex is suggested to poise the redox level and, consequently, optimizing the rate of cyclic electron transport under field conditions.

© 2009 Elsevier B.V. All rights reserved.

1. Introduction

The thylakoid Ndh complex is analogous to the NADH dehydrogenase or Complex I (EC 1.6.5.3) of the mitochondrial respiratory chain and catalyzes the transfer of electrons from NADH to plastoquinone [1–3]. Similarly to the mitochondrial Complex I and the cyanobacterial counterpart [4], the Ndh complex is L-shaped with the hydrophilic arm oriented towards stroma and the hydrophobic arm inserted into the thylakoid membrane. Eleven polypeptides of the Ndh complex (NDH polypeptides) are encoded by the plastid DNA *ndh* genes [5] and constitute the hydrophobic arm (NDH-A, -B, -C, -D, -E, -F and -G subunits) and part of the bridge between the two arms (NDH-H, -I, -J and -K subunits). Three nuclear encoded subunits (NDH-M, -N and -O) [3] probably form part of the bridge between the two arms. It is currently admitted that the Ndh complex includes additional yet to be identified nuclear encoded subunits harbouring the electron donor binding site in the arm oriented towards the stroma [6].

In concerted action with electron draining reactions, the Ndh complex protects against photo-oxidative-related stresses [7,8], probably by contributing to poise the redox level of the cyclic photosynthetic electron transporters [2,9]. By feeding excess electrons, over-expression of the *ndh* genes triggers the production of reactive oxygen species inducing programmed leaf cell death [10].

Results with *Arabidopsis* mutants [11] indicate that the nuclear encoded sigma4 factor favours the transcription of the *ndhF* gene by the plastid RNA polymerase. *ndhF* product could in turn stimulate the expression of the other plastid *ndh* genes. Further control mechanisms of transcript processing and translation increase the level of translatable monocystronic *ndh* transcripts under a variety of stress conditions [12–16]. Assays with barley indicate that, at the protein level, the NDH-F subunit also plays a key role controlling the Ndh complex activity increases by means of phosphorylation of a NDH-F subunit threonine [6,17]. Sequence comparison of the NDH-F polypeptide from different species [17] and immunodetection of tryptic peptides [4] indicated that the Thr-181, which is conserved in the plastid polypeptide but not in the Complex I homologous ND5/NuoL, is the likely phosphorylation target. Phosphorylation of abundant and hydrophilic polypeptides can easily be investigated through proteomic approaches [18]. In contrast, the difficulties involved in proteomic approaches to study phosphorylation of the Ndh complex, due to its low abundance in higher plant chloroplasts and the highly hydrophobic nature of its subunits, are well-known [19] and prompted us to attempt site-directed mutant approaches to validate the identification of the phosphorylation site, its presence in plants other than barley and the role of negative charge as determinant of the activation of the Ndh complex by phosphorylation. We have obtained three site-directed mutant transgenic tobaccos in which the $_{541}ACT_{543}$ triplet encoding the Thr-181 has been substituted by GCT, TCT or GAT encoding alanine, serine and aspartic acid, respectively. We compare Ndh activity, post-illumination chlorophyll fluorescence, photosynthesis activity and

---

* Corresponding author. Tel.: +34918854934; fax: +34918855066.
  E-mail address: bartolome.sabater@uah.es (B. Sabater).

morphological phenotypes of mutants and control plants demonstrating the key role of the Thr-181 phosphorylation in the activity and function of the Ndh complex.

2. Materials and methods

2.1. Plant culture

Callus of transformed tobacco (*Nicotiana tabacum*, cv. Petit Havana) was aseptically grown in vessels for sterile culture (Sigma V0633) on agar-solidified MS medium [20] supplemented with 30 g l^{-1} sucrose, 250 mg l^{-1} casein hydrolysate, 600 mg l^{-1} spectinomycin, 2.0 mg l^{-1} 2,4-dichlorophenoxyacetic acid (2,4-D) and 0.8% (w/v) agar, pH 5.8. For organogenesis, callus explants were transferred to a similar media except for the addition of 40 mg l^{-1} yeast extract and substituting 2,4-D with 1 mg l^{-1} 6-benzylaminopurine (BAP) and 0.1 mg l^{-1} naphthaleneacetic acid (NAA). Rooting was induced in plantlet explants by transfer to the same media without hormones. In vitro cultures were maintained at 23 °C under a 16-h photoperiod of 100 μmol photon m^{-2} s^{-1} of white light. After further 1–2 months in the aseptic rooting media, plantlets were transplanted to compost soil substrate in pots in a controlled glass house and irrigated with Murashige/Skoog. Seeds were obtained from regenerated plants that were regularly tested by sequencing 300–400 bases of the plastid DNA region around of the mutated site.

Seeds from transformed plants were aseptically germinated and seedlings grown in vessels for sterile culture (Sigma V0633) on agar-solidified MS medium [20] supplemented with 20 g l^{-1} sucrose, 250 mg l^{-1} casein hydrolysate, 600 mg l^{-1} spectinomycin and 0.8% (w/v) agar, pH 5.8. Cultures were maintained at 23 °C under a 16-h photoperiod of 100 μmol photon m^{-2} s^{-1} of white light. Plantlets as described above. Most assays were performed in plants derived from seeds. Some fluorescence and DNA assays were also repeated with callus-derived plants and always produced the same results as those from seeds.

Seeds from non-transformed *wt* tobacco were directly sown in pots with compost soil substrate, germinated and grown in the glass house.

2.2. Construction of vectors and transformation of tobacco

The sequence interval between nucleotide positions 111,594 and 112,032 of the tobacco plastid genome (GenBank accession number Z00044) was amplified by PCR (*Pfu*, Fermentas) with primers F1S.439 and F1SalI from tobacco plastid DNA and cloned into pGEM-T Vector System I (Promega). The resulting recombinant plasmid (pGEM-F1) was linearized with SacII and a PCR-product (primers: *aadA*.SacII.for and *aadA*.rev) of the *aadA* expression cassette [21] was introduced, yielding the plasmid pGEM-F1-*aadA*. A second sequence interval of the tobacco plastid genome (position 112,033–114,762) was amplified by PCR with primers F2_5′_AatII and F2AatIIrev and cloned into the AatII site in the pGEM-F1-*aadA* plasmid. The resulting plasmid pGEM-F1-*aadA*-F2 was sequenced for correct nucleotide sequence. For the codon substitutions in the *ndhF* gene changing the Thr-181 encoded in *wt* tobacco to Ala, Asp and Ser, the QuikChange Site-Directed Mutagenesis Kit (Stratagene) was used with the mutagenesis primers ndhF.T181A.for and ndhF.T181A.rev, ndhF.T181D.longfor and ndhF.T181D.longrev and ndhF.T181S.longfor and ndhF.T181S.longrev, respectively.

Leaves of 14-day-old sterile-grown tobacco seedlings were bombarded with plasmid DNA-coated gold particles using a biolistic gun (PDS-1000/He system, Bio-Rad, CA) and spectinomycin-resistant shoots were selected [22]. Plastid transformants were identified by PCR (*aadA* PCR (Primers: *aadA*re and *aadA*li59) and a PCR (A*ndhF* and F2AatIIrev) to check the mutation by sequencing the PCR-product with the primer A*ndhF*).

2.3. Isolation, amplification and sequencing of DNA

DNA was extracted from 0.5 g fresh or frozen specimens using either the protocol described by Tel-Zur et al. [23] or the DNeasy Plant Mini kit of Qiagen (GmbH, Hilden, Germany). DNA amplifications were performed using AccuPrime™ *Taq* DNA Polymerase (Invitrogen, GmbH, Lofer, Germany). PCR reaction mixtures were supplemented with 0.1% BSA (w/v) and 1% PVP (w/v) to release *Taq* DNA polymerase inhibitors present in nucleic acid preparations [24]. Cycling conditions were one cycle at 94 °C for 5 min and 35 cycles of 94 °C for 60 s, 46 °C for 60 s and 68 °C for 120–180 s. After agarose gel electrophoresis and purification (QIAquick Gel Extraction Kit, Qiagen) samples were sequenced on an Applied Biosystems automatic sequencer. Amplification and sequencing assays were carried out on 300–400 bases around the 541st position of the *ndhF* gene with the primers A*ndhF* on the PCR products resulting from the amplification with A*ndhF* and F2AatIIrev.

2.4. Extraction of the thylakoid Ndh complex, electrophoresis, zymograms and immunoassays

Leaves previously assayed for fluorescence induction were used to obtain a preparation of protein solubilized from thylakoids containing the Ndh complex. One g of leaf fragments was homogenized in a mortar with liquid N$_2$ and then with 3 ml of 50 mM potassium phosphate, pH7.0, 1 mM ascorbic acid, 1 mM EDTA-Na$_2$, 1%(w/v) polyvinyl pirrolidone and 2% Triton X-100. After gentle stirring for 5 min, the suspension was centrifuged at 20,000 ×g for 30 min. All steps were carried out between 0 and 5 °C. The supernatant containing, among other proteins, the thylakoid Ndh complex was immediately used for native electrophoresis and zymograms or stored at −20 °C for further assays [17].

If not otherwise indicated, native-PAGE was carried out with 75 μg protein at 5 °C in the presence of 0.1% Triton X-100 as described [17] in pre-formed Tris–HCl glycine, 4–15% acrylamide mini-gels, Bio-Rad, Hercules, CA, USA) for 3 h. NADH dehydrogenase zymograms were developed by incubating the gels for 1–2 h at room temperature in darkness with 50 mM potassium phosphate pH 8.0, 1 mM EDTA, 0.2 mM NADH, and 0.5 mg ml^{-1} nitroblue tetrazolium. In the control without NADH, no stain developed. The activity band corresponding to the Ndh complex was identified by immunoblotting [2].

SDS-PAGE was carried out with 80 μg protein at room temperature as described [17] in pre-formed 12% acrylamide mini-gels (Bio-Rad) for 35 min at 200 V. Gel proteins were revealed with Coomasie or processed for immunoblotting. For immunoblot analyses, proteins separated by native or SDS-PAGE were transferred to polyvinylidene difluoride membranes (PVDF) (Bio-Rad) as described [17]. NDH-A, NDH-D, NDH-F, NDH-J and NDH-K polypeptides were revealed using antibodies described previously [2,10,15–17]. Threonine phosphorylated polypeptides were immunodetected with mouse monoclonal anti-phospho-Thr (Sigma P3555). The different immunocomplexes were detected with the alkaline phosphatase western-blotting analysis system (Sigma) using the appropriate secondary antibody (anti-rabbit and anti-mouse Ig for, respectively, anti-Ndh polypeptides and anti-phospho-Thr).

Electrophoresis, zymograms and immunoassays were repeated at least three times.

2.5. Chlorophyll fluorescence induction analysis and measurement of net photosynthesis rate

Assays were carried out in the glass house with intact attached fully-expanded healthy leaves (containing around 25 μg chlorophyll cm^{-2}) of the mid-stem of tobacco plants at the beginning of flowering.

Chlorophyll fluorescence changes were measured with an Opti-Sciences (ADC BioScientific Ltd. Hertfordshire, UK) OS1-FL modulated

chlorophyll fluorometer at 28 °C in the green house after 4 h of daylight. Leaf disc regions were dark-adapted with clips for 30 min after which they received 2 min minimum light (0.1 μmol photon m^{-2} s^{-1} PAR) followed by 5 min higher relative light (0.15 μmol photon m^{-2} s^{-1} PAR) and 9 min again of minimum light. 0.8 s saturating flashes (5000 μmol photon m^{-2} s^{-1} PAR) were applied at 1, 3, 4, 5 and 6 min of light incubation. Fluorescence was recorded each 0.1 s and collected data were represented using the GraFit Erithacus software (Surrey, UK). Assays were repeated at least three times. The increase of fluorescence after relative high to minimum light transition is currently attributed to the reduction of plastoquinone mediated by the thylakoid Ndh complex [25–29]. Yield of quantum efficiency of light energy absorbed by photosystem II which is used in photosynthetic electron transport was calculated as $Y = (Fms - Fs) / Fms$ [28].

To measure net photosynthesis, appropriate leaf regions were fitted on the 6.25 cm^2 chamber of the LCpro+ portable photosynthesis system (ADC BioScientific Ltd. Hertfordshire, UK) equipped with the LED light unit and subjected, at 25 °C, 360 ppm CO_2 and environmental humidity (about 70%) to the following white light treatments (in μmol m^{-2} s^{-1} PAR): 15 min acclimation at 150 (130 at leaf surface) followed by 6 min successive periods at 1000 (870 at leaf surface), 70 (61 at leaf surface), 1000 (870 at leaf surface) and 150 (130 at leaf surface). Data collected each min and at light intensity transitions were directly represented using the GraFit Erithacus software (Surrey, UK).

2.6. Other determinations

Protein was determined by the Lowry method with Bio-Rad RC DC protein assay package. Chlorophyll was determined in intact leaves with the CCM-200 chlorophyll meter (ADC BioScientific Ltd. Herford-shiree, UK) with readings standarized for tobacco leaf chlorophyll determined by the Arnon method as described [28].

2.7. Oligonucleotides

| Oligonucleotide	Sequence (5′–3′)
F1S.439	CGGGGTACCGGTATTAGTCTGGATACGGC
F1SalI	ACGCGTCGACACAATTATAGCCTGTCTCTG
aadA.SacII.for	CGATCCGCGGGAATTCGCCGTCGTTCAATG
aadA.rev	CCCGGGTACCGAGCTCCACC
F2_5′_AatII	TACGACGTCTAGAATTTGCTAATCGGCTG
F2AatIIrev	TCAGACGTCAATTGTGAATTAAAAAAAACAG
ndhF.T181D.longfor	CTTGTCAAAAAGCGTTTGTAGATAATCGTGTAGGGGATTTTG
ndhF.T181D.longrev	CAAAATCCCCTACACGATTATCTACAAACGCTTTTTGACAAG
ndhF.T181S.longfor	CTTGTCAAAAAGCGTTTGTATCTAATCGTGTAGGGGATTTTG
ndhF.T181S.longrev	CAAAATCCCCTACACGATTAGATACAAACGCTTTTTGACAAG
ndhF.T181E.for	CTTGTCAAAAAGCGTTTGTAGAAAATCGTGTAGGGGATTTTG
ndhF.T181E.rev	CAAAATCCCCTACACGATTTTCTACAAACGCTTTTTGACAAG
ndhF.T181A.rev	CTACACGATTAGCTACAAACGC
ndhF.T181A.for	GCGTTTGTAGCTAATCGTGTAG
ndhF.T181D.longfor	CTTGTCAAAAAGCGTTTGTAGATAATCGTGTAGGGGATTTTG
ndhF.T181D.longrev	CAAAATCCCCTACACGATTATCTACAAACGCTTTTTGACAAG
ndhF.T181S.longfor	CTTGTCAAAAAGCGTTTGTATCTAATCGTGTAGGGGATTTTG
ndhF.T181S.longrev	CAAAATCCCCTACACGATTAGATACAAACGCTTTTTGACAAG
AndhF	TACGGTTGGAATTATGGTTC

3. Results

3.1. Construction and characterization of T181A, T181D and T181S mutants

The NDH-F subunit is a highly hydrophobic polypeptide probably located at the distal end of the hydrophobic arm of the thylakoid Ndh complex (Fig. 1C). Theoretic estimations and experimental tests suggest [6] that it consists of 15 transmembrane helices (Fig. 1A), exposing a large hydrophilic region (m) between helices XII and XIII to the lumen and a strong antigenic region (sequences $_{415}$WSKDEILSNSWLYS$_{428}$ in barley and $_{415}$WSKDEILNDSWLYS$_{428}$ in tobacco) between helices XI and XII to the stroma (Fig. 1A). The conserved and putatively phosphorylable Thr-181 is close to the
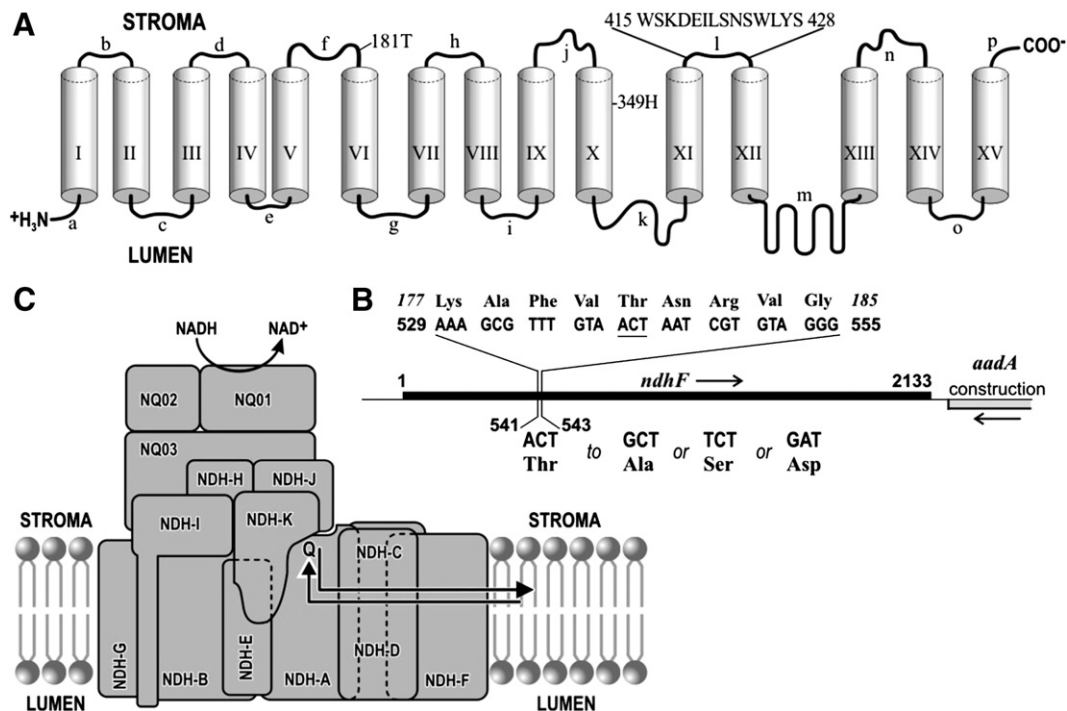
Fig. 1. Site-directed mutations in the *ndhF* gene. (A) Proposed transmembrane structure of the NDH-F polypeptide showing the position of the Thr-181 (181T) and the antigenic 415 to 428 amino acid sequence recognized by the NDH-F antiserum. (B) Base and encoded amino acid sequences around the ACT mutated codon and mutations changing the threonine encoded in *wt* tobacco. (C) Proposed structure of the Ndh complex in the thylakoid. Shaded subunits are encoded in chloroplast DNA. White subunits have not yet been identified and supposedly are encoded in nuclear DNA.
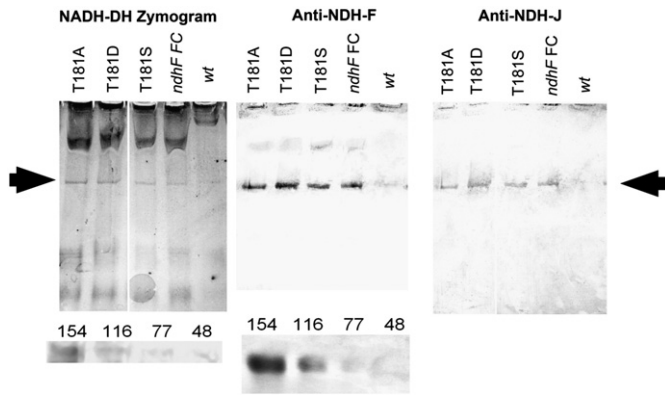
Fig. 2. Zymogram of NADH dehydrogenase activities and immunoblot identification of the Ndh complex. Solubilized thylakoid proteins from the indicated plants were separated by native electrophoresis and revealed for NADH dehydrogenase (NADH-DH) activity and, after membrane blotting, immunoassayed with antibodies against NDH-F and NDH-J polypeptides as indicated. The whole gel and membrane photos are shown to confirm the unambiguous identification of the activity (marked with arrow) corresponding to the Ndh complex as that containing proteins detected with NDH-F and NDH-J antibodies (arrow marks). Zymogram and anti-NDH-F dilution controls are shown below the respective plates for the indicated loading of protein (μg) solubilized from *wt* thylakoids.

transmembrane helix VI in the hydrophilic stroma-sided region f. A conserved His-349 in the X helix is probably involved in H+ pumping. Fig. 1B shows the codon substitutions changing the Thr-181 encoded in *wt* tobacco to Ala, Asp and Ser in, respectively, the T181A, T181D and T181S tobacco lines and the position of the *aadA* selecting gene 68 nucleotides down stream of the 3′ end of the modified *ndhF* gene.

Sequence profiles around the 542nd base of the *ndhF* in T181A, T181D and T181S tobacco lines and, for comparison, in *wt* and the control *ndhF* FC containing the *aadA* construction but no point base change, are in Supplementary materials (Fig. S1). As expected, with respect to controls, T181A and T181S have modified the codon to, respectively, GCT for Ala and TCT for Ser, which has been stably established for both transplastomic lines after three rounds of regeneration after the transformation. As for the T181D mutation, initially five lines were identified which showed at least a hetero-plastomic state for the codon 181 after two rounds of regeneration. In addition, a small T peak was found in two lines (namely 6/3 and 12/2) at the first position of codon 180 under the G encoded in the *wt* sequence. After two further rounds of regeneration, only two lines remained of which one (6/3) turned out to have lost the mutation in codon 181 completely. In contrast, the other line (12/2) not only maintained the mutation from ACT (Thr) to GAT (Asp) but also

revealed a second mutation at the first position of codon 180 leading to an amino acid exchange from Val to Leu. Interestingly, the only surviving lines had the small T peak already at early stages of the transformation process.

Repeated sequencing of the 300–400 bases surrounding the mutated base of all lines did not detect any other base change with respect to *wt* and *ndhF* FC lines. Routine sequencing indicated that all mutations were stable after four plant generations tested so far. Accordingly, the 180th and 181st amino acids predicted for *wt*, T181A, T181D and T181S lines are, respectively, ValThr, ValAla, LeuAsp and ValSer. As expected, the *ndhF* FC plants have the same amino acid sequence as *wt*.

No significant difference was found in the SDS-PAGE electrophoretic profile of the main polypeptides solubilized from thylakoids of the five tobacco lines (Supplementary Fig. S2).

3.2. Ndh activity

Freshly prepared extracts, containing the proteins solubilized from thylakoids with 2% Triton X-100, were subjected to native electrophoresis and tested for the reduction of nitroblue tetrazolium with NADH. The resulting zymograms (Fig. 2) showed several activity bands in the lanes corresponding to the six (T181A, T181D, T181S, *ndhF* FC and *wt*) tobacco lines assayed. The most intense bands must correspond to the most abundant NADH dehydrogenases and diaphorases present in thylakoids. The low-intensity band corresponding in each lane to the NADH dehydrogenase activity of the Ndh complex is unambiguously identified because, after subsequent transfer, it was exclusively recognized by both NDH-F and NDH-J antibodies as that migrating some 30% of the lane under the electrophoresis conditions. Clearly, the five plant lines contain, albeit in different amounts, the active Ndh complex, at least as NADH: nitroblue tetrazolium oxido-reductase.

Amino acid substitutions in T181A, T181D and T181S could affect both the relative enzymatic activity as well as the recognition of the NDH-F subunit by NDH-F antiserum. However, taking into account that the immuno-signal decreased more rapidly with sample dilution than the activity signal (see bottom of Fig 3), there is a good correspondence of the intensities of zymogram and immunodetection signals for each tobacco line. As *ndhF* FC and *wt* have the same NDH-F sequence, the ratio of *ndhF* FC/*wt* signals are similar (about 1.5) for zymogram and immunodetection with NDH-F and NDH-J antisera. The signals with anti-NDH-J are the most representative of the different levels of the Ndh complex in each plant line because the immunoreactivity of the NDH-J subunit is not affected by the site-directed mutations in the NDH-F subunit. In this respect, the level of
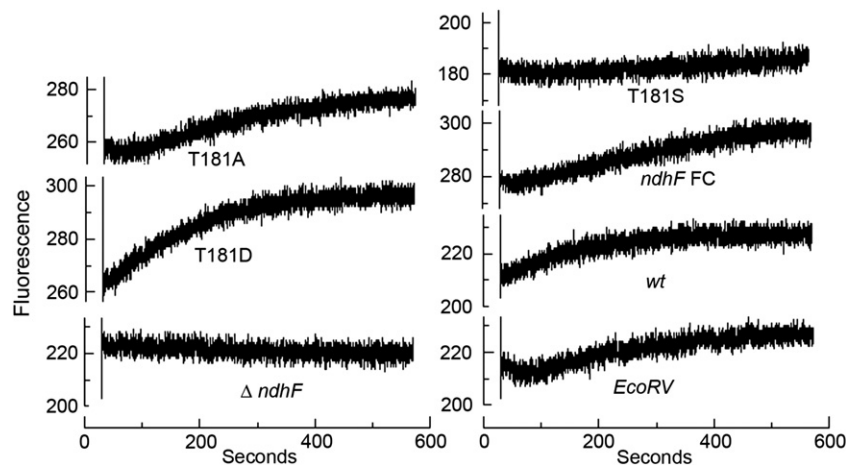
Fig. 3. Chlorophyll fluorescence traces after relative high to minimum light transition. Assays were performed as described in Materials and methods. The traces shown are only those of fluorescence readings every 0.1 s during the 9 min following the final 0.15 to 0.1 μmol photon m^{-2} s^{-1} PAR transition. Vertical axes show the relative fluorescence readings.

the Ndh complex was roughly similar in T181D and *ndhF* FC (and higher than in the other tobaccos), but the zymogram band is more intense in T181D than in *ndhF* FC, which suggests that substitution of Leu-180 and Asp-181 for Val-180 and Thr-181 increases the NADH: nitroblue tetrazolium oxido-reductase activity of the Ndh complex. Through a similar reasoning, as the almost equal level of the Ndh complex in T181A and T181S is lower than the level in *ndhF* FC and the intensity of the zymogram band is high in T181A and similar and relatively lower in T181S and *ndhF* FC, it may be speculated that the activity of the complex increases slightly when Thr-181 is substituted by Ser-181 and even more by Ala-181.

One of the main problems involved in the investigation of the structure–function relationships within the Ndh complex is that it rapidly becomes inactivated, losing activity and disintegrating into subunits, which, together with the scarcity of the complex in thylakoid extracts, impedes storage of sufficient amounts for analyses. To explore the possibility that any of the new NDH-F-modified Ndh complexes could have improved stability and also as an additional probe that genetic modifications in mutant tobaccos alter certain properties of the Ndh complex, zymograms and westerns with different NDH-polypeptide antibodies were assayed after native electrophoresis of the protein solubilized from thylakoids of the different tobaccos which had been stored for two months at −20 °C. The zymogram (Supplementary Fig. S3 and Supplementary Table SI) shows the loss of the band of Ndh activity in all extracts. Some low migrating and most fast migrating NADH dehydrogenase activities remained after two months, but none of them correspond to the Ndh complex. Although denatured, the Ndh complex or its subcomplexes were detected with specific antibodies for the remaining polypeptides. Only T181A and T181S extracts showed one or two bands with the five antisera assayed, which suggests that these two plants could provide modified Ndh complex or subcomplexes sufficiently stable for further investigations. By far, the Ndh complex of T181D was the least stable.

The effects of amino acid substitutions on the in vivo activity NADH:plastoquinone oxido-reductase of the Ndh complex could be different from the effects on the activity NADH:nitroblue tetrazolium oxido-reductase detected in zymograms, which limits the interest of the zymogram approach to compare the functional consequences of amino acid substitutions. The post-illumination increase of chlorophyll fluorescence is currently attributed to the reduction of plastoquinone mediated by the thylakoid Ndh complex [25–29] and could provide a complementary evaluation of the effects of amino acid substitutions on the in vivo activity of the Ndh complex. In order to obtain post-illumination fluorescence traces appropriate for a semi-quantitative estimation of rates of the increase of fluorescence, after five saturating flashes (Materials and methods) we select a small light intensity decrease (from 0.15 to 0.1 μmol photon m^{-2} s^{-1} PAR) after which fluorescence increases in leaves with functional Ndh complex.

As found previously for Δ*ndhF* tobacco [28], no significant difference was found in the quantum efficiency of photosystem II (ranging between 0.71 and 0.75) of the five tobacco lines which suggest that the photosynthetic electron transport was not affected in mutants.

Fig. 3 shows the fluorescence traces after the final relative high to minimum light transition of T181A, T181D, T181S, *ndhF* FC and *wt* tobaccos. In order to compare these results with the zymograms and immunodetection assays of Fig. 2, the fluorescence assays were carried out the day before the preparation of protein extracts of the same leaves. Both fluorescence assays and extract preparations began at midmorning, when plants in the glass house have received around 4 h of daylight. For a comparison, Fig. 3 also includes the fluorescence traces of the transgenic tobaccos Δ*ndhF* and *EcoRV* previously described [10,28]. Δ*ndhF* tobacco contains an inactivated *ndhF* gene by insertion of the *aadA* construction in the open reading frame; *EcoRV* is a control transgenic tobacco including the *aadA* cassette in an intergenic region of plastid DNA. We reported that Δ*ndhF* lacks Ndh

complex and does not show the post-illumination increase of chlorophyll fluorescence [28]. In contrast, no difference has been found between *wt* and *EcoRV* tobacco. In agreement with previous results, Fig. 3 shows that Δ*ndhF* did not show the increase of fluorescence in the new fluorescence assay after decrease of light intensity (in fact, it shows a slight decrease of fluorescence). In contrast, *EcoRV* shows the characteristic Ndh-dependent increase of fluorescence. Accordingly, the assay conditions seem appropriate to detect and roughly estimate the activity of the Ndh complex transferring electrons to plastoquinone in vivo.

Fig. 3 shows that T181A, *ndhF* FC and *wt* tobaccos had similar fluorescence increases after transition to low light. Fluorescence increase was almost absent in T181S, which suggests that although the NADH:nitroblue tetrazolium oxido-reductase activity of the Ndh complex is not sensibly affected (Fig. 2), the substitution of Ser for Thr-181 could strongly impair the NADH:plastoquinone oxido-reductase activity. The high increase of fluorescence of T181D could be due to both a high level of the complex in the T181D tobacco and an enhancement of the NADH:plastoquinone oxido-reductase activity of the complex when Val-180 and Thr-181 are substituted by Leu-180 and Asp-181. This possibility would suggest that the negative charge of the Asp-181 simulates the hypothetical activation of the *wt* complex by phosphorylation of the Thr-181 in T181D tobacco.

3.3. Photosynthesis rate responses to rapid changes of light intensity

The Ndh complex provides electrons to poise the redox level of the intermediaries of cyclic electron transport [2] when rapid decreases in light intensity transitorily reduce the electron supply from photosystem II. Hence, probably, proper activation of the Ndh complex would improve the photosynthetic performance under rapid changes of the light intensity. To test this hypothesis and the potential involvement of the Thr-181 phosphorylation in the photosynthetic responses to rapid changes of light intensity, we compared the CO_2 consumption rate of leaves of control and mutant plants subjected to rapid transitions of light intensity (sequential 6 min periods of 870, 61, 870 and 130 μmol photon m^{-2} s^{-1} PAR after a 15 min acclimation period at 130 μmol photon m^{-2} s^{-1} PAR). T181A showed (Fig. 4) the lowest rates of net photosynthesis and a slow adaptation of the photosynthesis rate when light intensity changes from 870 to 61 and from 61 to 870 μmol photon m^{-2} s^{-1} PAR. In contrast, *wt*, *ndhF* FC and T181D showed rapid changes of photosynthesis rates in response to variation of light intensity and significantly higher rates of mean photosynthesis, around 5.5 to 6 μmol CO_2 fixed m^{-2} s^{-1} than T181A (4 μmol CO_2 fixed m^{-2} s^{-1}). In agreement with the role of the thylakoid Ndh complex, after the transition of 61 to 870 μmol photon m^{-2} s^{-1} PAR, the rate of photosynthesis increased slowly in Δ*ndhF* reaching a maximum after 6 min. Although starting from a slightly lower rate of photosynthesis at 61 μmol photon m^{-2} s^{-1} PAR, the recovery of the high photosynthesis rate when light abruptly increased to 870 μmol photon m^{-2} s^{-1} PAR was quicker (approximately a 1 min delay) in T181D than in controls *wt* and *ndhF* FC (2 min delay). A limited number of assays (not shown) with T181S tobacco produced results similar to Δ*ndhF* and T181A. It seems that in some way, the impossibility of Thr-181 phosorylation impairs the photosynthesis performance in T181A under rapidly fluctuating light intensities. Similarly, the negative charge of the Asp-181 in T181D tobacco simulates the activation of the *wt* complex by phosphorylation of the Thr-181 resulting in an even quicker recovery of photosynthesis rate when light increases from 61 to 870 μmol photon m^{-2} s^{-1} PAR.

3.4. The NDH-F subunit is not phosphorylated in site-directed mutants

The phosphorylation of the NDH-F subunit was detected in barley [17] by the co-migration in SDS-PAGE of a polypeptide revealed with
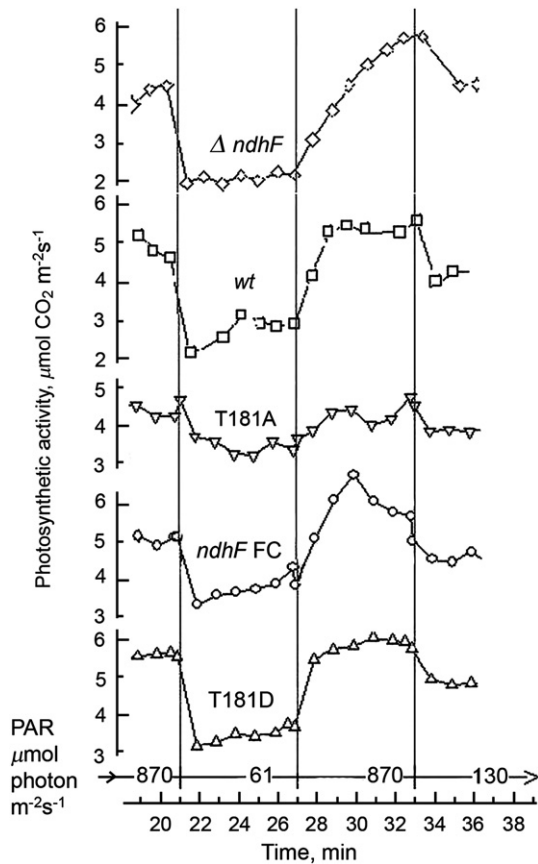
Fig. 4. Photosynthetic responses to rapid changes of light intensity. After 15 min acclimation to 130 μmol photon m^{-2} s^{-1} PAR, the rate of net photosynthesis (as μmol CO_2 fixed m^{-2} s^{-1}, vertical axes) was monitored each min and in the transitions of light intensity in full expanded healthy leaves (25 μg chlorophyll cm^{-2}) of $\Delta ndhF$, *wt*, T181A, *ndhF* FC and T181D tobaccos receiving sequential 6 min periods of 870, 61, 870 and 130 μmol photon m^{-2} s^{-1} PAR as indicated in horizontal axes. No significant difference in the response curve for each tobacco was found in experiments at least twice repeated.

NDH-F antiserum and a polypeptide revealed with monoclonal phospho-threonine antibody. Now, we performed native- and SDS-PAGE western assays with the polypeptides solubilized from thylakoids of different tobaccos. Western and immunoassay after native-PAGE (Fig. 5A) detected the presence of phospho-threonine containing band in *ndhF* FC, but not in T181A, T181D and T181S thylakoids. Comparison with band migration in Fig. 3 and immunoassay with NDH-F and NDH-J antibodies (Fig. 5A) of lanes run in parallel strongly suggest that the phospho-threonine signal of *ndhF* FC corresponds to the Ndh complex. After SDS-PAGE and western, Fig. 5B shows that anti-phospho-threonine revealed the presence of several polypeptides in all tobacco lines; among them a polypeptide of Mr around 65 kD. Probably, several threonine phosphorylated peptides detected after SDS-PAGE run out of the gel and were not detected after the longer running of native-PAGE. A polypeptide of slightly higher Mr, around 73 kD, co-migrating with the NDH-F polypeptide detected with anti-NDH-F in the *ndhF* FC extract, was clearly detected with anti-phospho-Thr in the *ndhF* FC extract and barely detected in the *wt* extract (Fig. 5B). The higher level of the 73 kD phosphorylated polypeptide in the *ndhF* FC than in the *wt* extract coincides with the relative abundance detected with anti-NDH-F in the two plants (Fig. 2). It is noteworthy that the 73 kD phosphorylated polypeptide was not detected in T181A, T181D and T181S lanes (Fig. 5), which provides strong genetic support to previous suggestions [6,17] that the Thr-181 is the amino acid phosphorylated for the activation of the Ndh complex. If antibody sensitivity and Ndh complex extractability are

not very different in the tobacco lines, the absence of the 73 kD phosphorylated polypeptide in any of the T181A, T181D and T181S lines can only be attributed to the substitution of the Thr-181 by, respectively, the non-phosphorylable Ala-181, Asp-181, Asp-181 and Ser-181.

4. Discussion

Site-directed mutagenesis is a powerful approach to identify phosphorylation sites in polypeptides, the charge-related effect of phosphorylation on the activity of the protein and the functional consequences of specific phosphorylations in the organism. It is particularly useful to investigate regulatory proteins which, like those involved in signal transduction [30–32], are present below the minimal concentration required in other approaches. Even for abundant proteins, site-directed mutagenesis of the photosystem II D2 polypeptide permitted the identification of the threonine residue at position 2 as the target for phosphorylation in *Chlamydomonas reinhardtii* [33]. Similarly, site-directed mutants affecting the *Escherichia coli* Complex I revealed the involvement of two lysine residues of the NuoM subunit (homologous to the NDH-D subunit of the thylakoid Ndh complex) in proton pumping [34] and of Glu-95 of the NuoF subunit (homologous to the hypothetical NQO1 of Fig. 1C) affecting the kinetic properties and redox potential of the subunit [35]. In a different approach, site-directed mutants of the *Zea mays* sucrose synthase gene expressed in *E. coli* allowed the identification of the serine at position 15 as that controlling the membrane association of the enzyme [36]. The low abundance of Ndh complex in higher plant chloroplasts (approximately 1 for each 100 to 200 photosystem subunits, [1,10]) and difficulties involved in the proteomic handling of highly hydrophobic subunits [19] such as NDH-F justify the site-directed mutant approach to further investigate its phosphorylation.

Immunoassays (Fig. 5) detected the 73 kD phosphorylated polypeptide in *wt* and *ndhF* FC, but not in any of the site-directed mutants (T181A, T181D and T181S) tested. The results obtained by site-directed mutagenesis in tobacco confirm that the Thr-181 is the amino acid phosphorylated in vivo, as suggested the protease digestion assays with the NDH-F subunit of barley [6,17]. Extensive searching in data banks (not shown) indicated that this residue and neighbouring amino acids are conserved in all higher plant NDH-F subunits but not in the homologous NuoL subunit of respiratory complex I. Although a homologous threonine is present in the NDH-F of the cyanobacteria *Synechocystis*, the neighbouring amino acid sequences are very different from those in higher plants, which are highly conserved. This suggests that the evolutionary appearance of the Thr-181 phosphorylation could be restricted to the branch leading to terrestrial plants.

The NADH:nitro blue tetrazolium oxido-reductase activity of the thylakoid Ndh complex can be unambiguously distinguished, among major faster and lower migrating activities, as a small band migrating about 30% of the lane which reacts with antibodies against NDH-F and NDH-J polypeptides (Fig. 2). The good correspondence between the intensity of the bands for two western signals and the zymogram signal for each plant further supports the identification of the activity band corresponding to the Ndh complex. Despite minor differences, the results shown in Fig. 2 indicate that the three site-directed mutants T181A, T181D and T181S have NADH:nitro blue tetrazolium oxido-reductase activity. Accordingly, structural analyses (secondary structure and disorder prediction carried out at http://swissmodel. expasy.org [37]) did not detect significant differences in the NDH-F structure of *wt* and mutants (not shown). However, the steady-state level of the Ndh complex varies among the mutants (Fig. 2).

Under the assay conditions of Fig. 3, the chlorophyll fluorescence rise after light decrease plausibly provides a semi-quantitative estimation of the NADH:plastoquinone oxido-reductase activity of
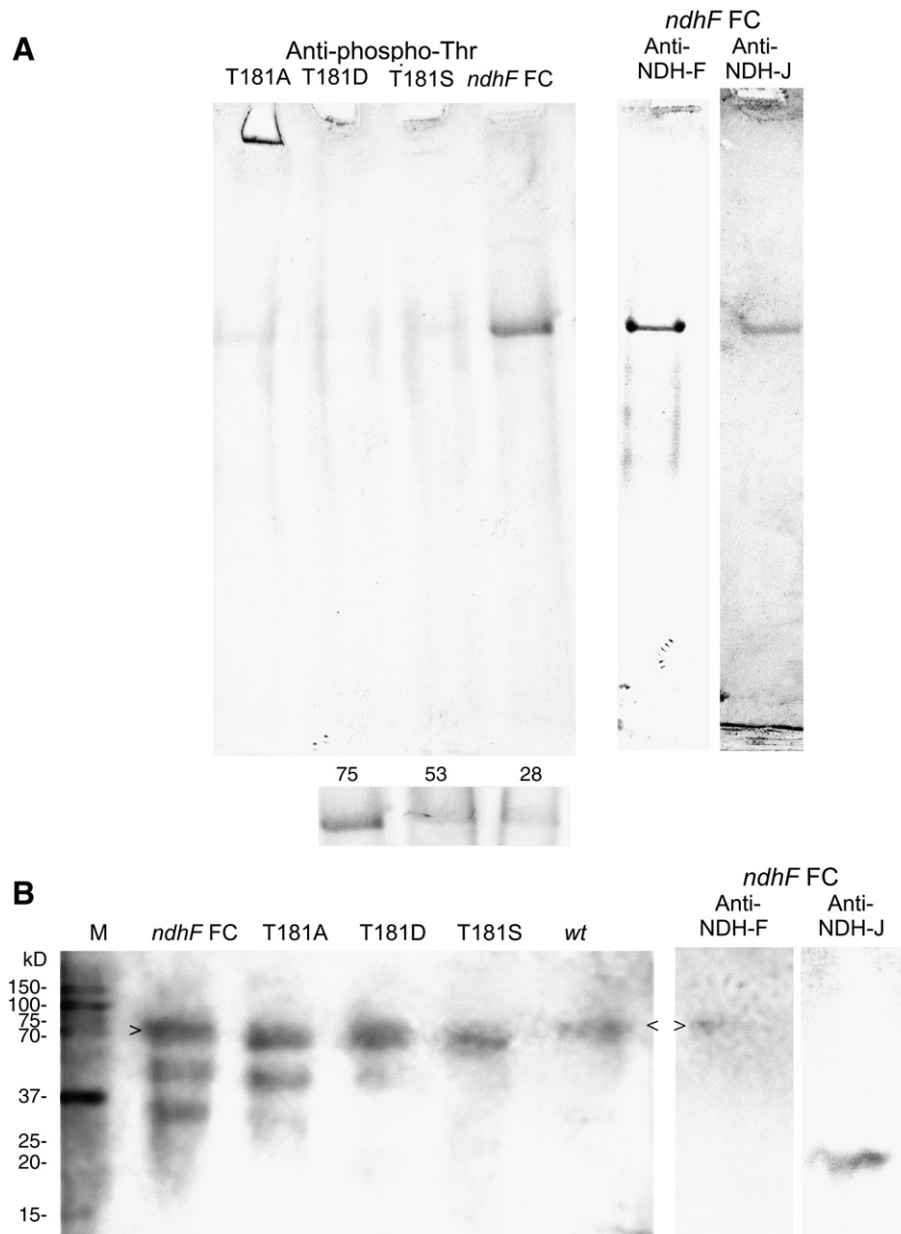
Fig. 5. The NDH-F polypeptide is not phosphorylated in mutant tobaccos. Thylakoid polypeptides solubilized from the indicated plants were subjected to native-PAGE (A) and SDS-PAGE (B) and western-blot analysis using phospho-Thr, NDH-F and NDH-J antibodies as indicated. In A, anti-phospho-Thr dilution controls of protein (μg) solubilized from *ndhF* FC thylakoids are shown below together the same 75 μg band. In B, angles point the 73 kD bands detected by phospho-Thr and NDH-F antibodies and size markers are shown on the left.

the Ndh complex truly acting in vivo. In this regard, notable differences were evident among the site-directed mutants that cannot be only explained on the basis of differences in the level of the Ndh complex. Substitution of alanine for threonine in the T181A mutant did not sensibly affect the actual fluorescence rise in *wt* and *ndhF* FC plants. However, the serine for threonine substitution in T181S almost entirely suppressed fluorescence rise (Fig. 3), although the complex level in T181S was comparable to that in T181A and *ndhF* FC.

By far, substitution of aspartic acid for threonine in T181D had the most dramatic effect on the level, the activity of the complex and on the fluorescence rise. As explained in the Results section, the high rate fluorescence rise in T181D cannot only be based on higher protein level and the result shown in Fig. 3 indicated that substitution of aspartic for threonine in T181D results in a Ndh complex with increased NADH:plastoquinone oxido-reductase activity, which strongly suggests that the negative charge of the dissociated Asp-181 in T181D mimics the activation effect of the

threonine phosphorylation in the Ndh complex of *wt* tobacco. It seems plausible that, under the fluorescence assay conditions, the Ndh complex of *wt* did not reach full phosphorylation and activation, while the stable high activity in T181D endowed it a rapid fluorescence response. A similar effect of negative charge due to aspartic or glutamic acids mimicking the phosphorylation of serine or threonine residues in *wt* proteins were reported in the abscisic acid-dependent activation of the transcription factor AREB1 [31] and in the binding of the sucrose synthase to membranes dependent on Ser-15 phosphorylation [36] which is suppressed when alanine was substituted for phosphorylable serine. In this regard, the fluorescence response of T181A, T181D and T181S supports the earlier conclusion with the Ndh complex of barley that the phosphorylation of the Thr-181 of the NDH-F subunit stimulates the activity of the complex. The substitution of acidic amino acids for Thr-2 was reported to drastically impair the synthesis/accumulation of D2 polypeptide of photosystem II in *Chlamydomonas reinhardtii* [33]. A similar effect

could explain the behaviour of the complex level differences among tobacco mutants.

It was hypothesized that, in higher plants, the Ndh complex provides electrons to poise the redox level of the intermediaries of cyclic electron transport [2] participating as an entry valve in a chlororespiratory electron transport chain where the Mehler reaction, superoxide dismutase, plastoquinol peroxidase and plastid terminal oxidase [38] would drain the excess of electrons. Several stresses, such as extreme temperatures, rapid changes in light intensity and low water (which, by closing stomata, decreases CO_2 availability), strongly affect the rates of both electron supply from photosystem II and electron consumption in the Calvin cycle, therefore requiring rapid redox poising in order to maintain the cyclic electron transport functional. Accordingly, several stresses were reported to increase the level and activity of the Ndh complex [28] (and references herein). Rapid activation of the Ndh valve is accomplished by phosphorylation of the NDH-F subunit [17] as the final stage of a signal transduction involving H_2O_2 [12]. Under conditions of high activity of the Ndh complex that are not accompanied by a similar higher level of the electron draining reactions, such as superoxide dismutase [39,40], the production of reactive oxygen species increases [10] triggering leaf senescence.

The most obvious primary role of the Ndh complex is to improve the photosynthetic performance under field conditions. Although mutation does not affect the photosynthetic electron transport from photosystem II, the rapid changes of light intensity reveal strong differences of carbon fixation activity among T181A, *ndhF* FC control and T181D (Fig. 4). T181A shows a low capability to adapt photosynthesis rates to changing light intensities. The overall effect of this deficiency during the time assay shown in Fig. 4 decreases approximately 20% net photosynthesis of T181A in respect to *ndhF* FC and T181D. It seems plausible that, in the windy field, where one leaf is subjected to transitory shadowing (lasting a few seconds) by other leaves or by clouds, the shorter duration of the different periods and the larger differences in light intensity could impair further the photosynthesis rate in T181A. The 1 min minimum span between successive data captures by the portable photosynthesis apparatus limits the possibilities to confirm this. Less spectacular but also significant is the quicker response of T181D compared to *ndhF* FC in the photosynthesis rate when light increases from 61 to 870 μmol photon m^{-2} s^{-1} PAR (Fig. 4). As pointed out in Results, the slow adaptation of T181A to changing light intensities seems due to the impossibility of Ndh activation by Thr-181 phosphorylation. Consequently, the negative charge of the Asp-181, simulating the *wt* complex activation by phosphorylation, could explain a quicker recovery of the photosynthesis rate in T181D tobacco than in *ndhF* FC. Another question refers to the mechanism by which the poising of electron transporters by the active Ndh complex feeding of electrons improves the rate of CO_2 assimilation. Under the assay conditions of Fig. 4, at the end of the first 6 min period at 870 μmol photon m^{-2} s^{-1} PAR (that follows the 15 min acclimation period at 130 μmol photon m^{-2} s^{-1} PAR) the photosynthesis rate is stabilized and, plausibly, photosystem II is partially photoinhibited. Sudden transition to 61 μmol photon m^{-2} s^{-1} PAR reduces the flow of electrons from photosystem II while the active Calvin cycle drains them. In the absence of Ndh activity, the consequent over-oxidation of intermediaries would collapse cyclic electron transport and photophosphorylation. Under these conditions, ATP availability should be the limiting factor for the Calvin cycle at the beginning of the following 870 μmol photon m^{-2} s^{-1} PAR period and the rate of CO_2 fixation would only slowly recover. Active Ndh complex would prevent the over-oxidation of intermediaries during the 61 μmol photon m^{-2} s^{-1} PAR period, ensuring photophosphorylation and the rapid recovery of CO_2 fixation rates in the subsequent 870 μmol photon m^{-2} s^{-1} PAR period. Measurements of ATP and NADPH levels, fluorescence and CO_2 fixation rates in the different mutants at shorter intervals during

fluctuating light could provide further clues on the significance of the Ndh complex for terrestrial photosynthesis where rapid changes of light intensity, temperature and stomata opening strongly affect the rates of feeding and draining of electrons in photosynthetic electron transport chain.

All together, photosynthesis-related traits of the site-directed mutants reported here strongly suggest the requirement of a thylakoid Ndh complex phosphorylable at the Thr-181 of the NDH-F subunits for optimal photosynthetic performance under field conditions.

Appendix A. Supplementary data

Supplementary data associated with this article can be found, in the online version, at doi:10.1016/j.bbabio.2009.03.001.

References

[1] L. Sazanov, P.A. Burrows, P.J. Nixon, The plastid ndh genes code for a NADH-specific dehydrogenase: purification and characterization of a mitochondrial-like complex I from pea thylakoid membranes, Proc. Natl. Acad. Sci. U. S. A. 95 (1998) 1319–1324.
[2] L.M. Casano, J.M. Zapata, M. Martín, B. Sabater, Chlororespiration and poising of cyclic electron transport: plastoquinone as electron transporter between thylakoid NADH dehydrogenase and peroxidase, J. Biol. Chem. 275 (2000) 942–948.
[3] D. Rumeau, N. Becuwe-Linka, A. Beyly, M. Louwagie, J. Garin, G. Peltier, New subunits NDH-M, -N, and -O, encoded by nuclear genes, are essential for plastid Ndh complex functioning in higher plants, Plant Cell 17 (2005) 219–232.
[4] P. Prommeenate, A.M. Lennon, C. Markert, M. Hipler, P. Nixon, Subunit composition of NDH-1 complexes of *Synechocystis* sp. PCC 6803, J. Biol. Chem. 279 (2005) 28165–28173.
[5] R.M. Maier, K. Neckermann, G.L. Igloi, H. Kössel, Complete sequence of the maize chloroplast genome: gene content, hotspots of divergence and fine tuning of genetic information by transcript editing, J. Mol. Biol. 251 (1995) 614–628.
[6] L.M. Casano, H.R. Lascano, M. Martín, B. Sabater, Topology of the plastid Ndh complex and its NDH-F subunit in thylakoid membranes, Biochem. J. 382 (2004) 145–155.
[7] M. Martín, L.M. Casano, B. Sabater, Identification of the product of *ndhA* gene as a thylakoid protein synthesized in response to photooxidative treatment, Plant Cell Physiol. 37 (1996) 293–298.
[8] T. Endo, T. Shikanai, A. Takabayashi, K. Asada, F. Sato, The role of chloroplastic NAD(P)H dehydrogenase in photoprotection, FEBS Lett. 457 (1999) 5–8.
[9] T. Joët, L. Cournac, G. Peltier, M. Havaux, Cyclic electron flow around photosystem I in C3 plants. In vivo control by the redox state of chloroplast and involvement of the NADH-dehydrogenase complex, Plant Physiol. 128 (2002) 760–769.
[10] J.M. Zapata, A. Guéra, A. Esteban-Carrasco, M. Martín, B. Sabater, Chloroplasts regulate leaf senescence: delayed senescence in transgenic *ndhF*-defective tobacco, Cell Death Differ. 12 (2005) 1277–1284.
[11] J.J. Favory, M. Kobayshi, K. Tanaka, G. Peltier, M. Kreis, J.G. Valay, S. Lerbs-Mache, Specific function of a plastid sigma factor for *ndhF* gene transcription, Nucleic Acids Res. 33 (2005) 5991–5999.
[12] L.M. Casano, M. Martín, B. Sabater, Hydrogen peroxide mediates the induction of chloroplast Ndh complex under photooxidative stress in barley, Plant Physiol. 125 (2001) 450–1458.
[13] E.M. Del Campo, B. Sabater, M. Martín, Transcripts of the *ndhH-D* operon of barley plastids: possible role of unedited site III in splicing of the *ndhA* intron, Nucleic Acids Res. 28 (2000) 1092–1098.
[14] E.M. Del Campo, B. Sabater, M. Martín, Post-transcriptional control of chloroplast gene expression: accumulation of stable psaC mRNA is due to downstream RNA cleavages in the *ndhD* gene, J. Biol. Chem. 277 (2002) 36457–36464.
[15] E.M. Del Campo, B. Sabater, M. Martín, Characterization of the 5′- and 3′-ends of mRNAs of *ndhH*, *ndhA* and *ndhI* genes of the plastid *ndhH-D* operon, Biochimie 88 (2006) 347–357.
[16] P.H. Serrot, B. Sabater, M. Martín, Expression of the ndhCKJ operon of barley and editing at the 13th base of the mRNA of the ndhC gene, Biol. Plant. 52 (2008) 347–350.
[17] H.R. Lascano, L.M. Casano, M. Martín, B. Sabater, The activity of the chloroplastic Ndh complex is regulated by phosphorylation of the NDH-F subunit, Plant Physiol. 132 (2003) 256–262.
[18] G. Del Riego, L.M. Casano, M. Martín, B. Sabater, Multiple phosphorylation sites in the β subunit of thylakoid ATP synthase, Photosynth. Res. 89 (2006) 11–18.

[19] C.C. Darie, M.L. Biniossek, V. Winter, B. Mutschler, W. Haehnel, Isolation and structural characterization of the Ndh complex from mesophyll and bundle sheath chloroplasts of *Zea mays*, FEBS J. 272 (2005) 2705–2716.

[20] T. Murashige, F. Skoog, A revised medium for rapid growth and bio-assays with tobacco tissue cultures, Physiol. Plant 15 (1962) 473–497.

[21] H.U. Koop, K. Steinmuller, H. Wagner, C. Rossler, C. Eibl, L. Sacher, Integration of foreign sequences into the tobacco plastome via polyethylene glycol-mediated protoplast transformation, Planta 199 (1996) 193–201.

[22] Z. Svab, P. Maliga, High-frequency plastid transformation in tobacco by selection for a chimeric *aadA* gene, Proc. Natl. Acad. Sci. U. S. A. 90 (1993) 913–917.

[23] N. Tel-Zur, S. Abbo, D. Myslabodski, Y. Mizrahi, Modified CTAB Procedure for DNA Isolation from Epiphytic Cacti of the General *Hylocereus* and *Selenicereus* (Cactaceae), Plant Mol. Biol. Rep. 17 (1999) 249–254.

[24] Z. Xin, J.P. Velten, M.J. Oliver, J.J. Burke, A simple versatile high throughput DNA extraction method suitable for PCR, Biotechniques 34 (2003) 820–826.

[25] P.A. Burrows, L.A. Sazanov, Z. Svab, P. Maliga, P.J. Nixon, Identification of a functional respiratory complex in chloroplasts through analysis of tobacco mutants containing disrupted plastid *ndh* genes, EMBO J. 17 (1998) 868–876.

[26] W. Kofer, H.U. Koop, G. Wanner, K. Steinmüller, Mutagenesis of the genes encoding subunits A, C, H, I, J, and K of the plastid (NAD(H)-plastoquinone-oxidoreductase in tobacco by polyethylene glycol-mediated plastome transformation, Mol. Gen. Genet. 258 (1998) 166–173.

[27] T. Shikanai, T. Endo, T. Hashimoto, Y. Yamada, K. Asada, A. Yokota, Directed disruption of the tobacco ndhB gene impairs cyclic electron flow around photosystem I, Proc. Natl. Acad. Sci. U. S. A. 95 (1998) 9705–9709.

[28] M. Martín, L.M. Casano, J.M. Zapata, A. Guéra, E.M. Del Campo, C. Schmitz-Linneweber, R.M. Maier, B. Sabater, Role of thylakoid Ndh complex and peroxidase in the protection against photo-oxidative stress: fluorescence and enzyme activities in wild-type and *ndhF*-deficient tobacco, Physiol. Plant 122 (2004) 443–452.

[29] D. Wang, A.R. Portis, A novel nucleus-encoded chloroplast protein, PIFI, is involved in NAD(P)H dehydrogenase complex-mediated chlororespiratory electron transport in *Arabidopsis*, Plant Physiol. 144 (2007) 1742–1752.

[30] J.I. Kim, J.E. Park, X. Zarate, P.S. Songa, Phytochrome phosphorylation in plant light signalling, Photochem. Photobiol. Sci. 4 (2005) 681–687.

[31] T. Furihata, K. Maruyama, Y. Fujita, T. Umezawa, R. Yoshida, K. Shinozaki, K. Yamaguchi-Shinozaki, Abscisic acid-dependent multisite phosphorylation regulates the activity of a transcription activator AREB1, Proc. Natl. Acad. Sci. U. S. A. 103 (2006) 1988–1993.

[32] N.L. Weigel, N.L. Moore, Kinases and protein phosphorylation as regulators of steroid hormone action, Nucl. Recep. Sign. 17 (5) (2007) e005.

[33] M.M. Fleischmann, J.D. Rochaix, Characterization of mutants with alterations of the phosphorylation site in the D2 photosystem II polypeptide of *Chlamydomonas reinhardtii*, Plant Physiol. 119 (1999) 1557–1566.

[34] L. Euro, G. Belevich, M.I. Verkhovsky, M. Wikström, M. Verkhovskaya, Conserved lisine residues of the membrane subunit NuoM are involved in energy conversión by proton-pumping NADH:ubiquinone oxidoreductase (Complex I), Biochim. Biophys. Acta 1777 (2008) 1166–1172.

[35] L. Euro, G. Belevich, D.M. Bloch, M.I. Verkhovsky, M. Wikström, M. Verkhovskaya, The role of the invariant glutamate 95 in the catalytic site of Complex I from *Escherichia coli*, Biochim. Biophys. Acta 1787 (2009) 68–73.

[36] S.C. Hardin, H. Winter, S.C. Huber, Phosphorylation of the amino terminus of maize sucrose synthase in relation to membrane association and enzyme activity, Plant Physiol. 134 (2004) 1427–1438.

[37] E.M. Zdobnov, R. Apweiler, InterProScan — an integration platform for the signature-recognition methods in InterPro, Bioinformatics 17 (2001) 847–848.

[38] D. Rumeau, G. Peltier, L. Cournac, Chlororespiration and cyclic electron flow around PSI during photosynthesis and plant stress response, Plant Cell Environ. 30 (2007) 1041–1051.

[39] L.M. Casano, M. Martín, B. Sabater, Sensitivity of superoxide dismutase transcript levels and activities to oxidative stress is lower in mature-senescent than in young barley leaves, Plant Physiol. 106 (1994) 1033–1039.

[40] D. Abarca, M. Martín, B. Sabater, Differential leaf stress responses in young and senescent plants, Physiol. Plant. 113 (2001) 409–415.